Quantification of calcium signal transmission from sarco-endoplasmic reticulum to the mitochondria

Pál Pacher, György Csordás, Timothy G. Schneider and György Hajnóczky

Department of Pathology, Anatomy and Cell Biology, Thomas Jefferson University, Philadelphia, PA 19107, USA

(Received 16 May 2000; accepted after revision 1 September 2000)

1. Recent studies have shown that ryanodine and IP_3 receptor (RyR/IP_3R)-mediated cytosolic Ca^{2+} signals propagate to the mitochondria, initiating chains of events vital in the regulation of different cellular functions. However, the fraction of released Ca^{2+} utilized by the mitochondria during these processes has not been quantified.

2. To measure the amount of Ca^{2+} taken up by the mitochondria, we used a novel approach that involves simultaneous fluorescence imaging of mitochondrial and cytosolic [Ca^{2+}] in permeabilized H9c2 myotubes and RBL-2H3 mast cells. Communication between sarco-endoplasmic reticulum (SR/ER) and mitochondria is maintained in these permeabilized cells, as evidenced by the large RyR/IP_3R-driven mitochondrial matrix [Ca^{2+}] and NAD(P)H signals and also by preservation of the morphology of the SR/ER-mitochondrial junctions.

3. Ca^{2+} was released from the SR/ER by addition of saturating caffeine or IP_3 and subsequently thapsigargin (Tg), an inhibitor of SR/ER Ca^{2+} pumps. The amount of Ca^{2+} transmitted to the mitochondria was determined by measuring increases of global [Ca^{2+}] in the incubation medium (cytosolic [Ca^{2+}] ([Ca^{2+}]$_c$)). Mitochondrial Ca^{2+} uptake was calculated from the difference between [Ca^{2+}]$_c$ responses recorded in the absence and presence of uncoupler or from [Ca^{2+}]$_c$ elevations evoked by uncoupler or ionophore applied after complete Ca^{2+} mobilization from the SR/ER. [Ca^{2+}]$_c$ increases were calibrated by adding Ca^{2+} pulses to the permeabilized cells.

4. In H9c2 cells, caffeine induced partial mobilization of SR Ca^{2+} and mitochondria accumulated 26% of the released Ca^{2+}. Sequential application of caffeine and Tg elicited complete discharge of SR Ca^{2+} without further increase in mitochondrial Ca^{2+} uptake. In RBL-2H3 mast cells, IP_3 by itself elicited complete discharge of the ER Ca^{2+} store and the increase of the ionophore-releasable mitochondrial Ca^{2+} content reached 50% of the Ca^{2+} amount mobilized by IP_3 + Tg. Thus, RyR/IP_3R direct a substantial fraction of released Ca^{2+} to the mitochondria.

Increasing evidence suggests that mitochondria are important in intracellular Ca^{2+} signalling (for recent reviews see Babcock & Hille, 1998; Jouaville *et al.* 1998; Simpson & Russell, 1998; Duchen, 1999; Rizzuto *et al.* 1999; Hajnóczky *et al.* 2000; Hüser *et al.* 2000). It has been shown that cytosolic calcium signals elicited by activation of IP_3R or RyR are transmitted to the mitochondria (Rizzuto *et al.* 1993, 1998; Hajnóczky *et al.* 1995; Chacon *et al.* 1996; Drummond & Tuft, 1999). Mitochondrial Ca^{2+} content measured by different techniques has also been shown to be elevated in cells exposed to Ca^{2+} mobilizing agonists (e.g. Wendt-Gallitelli & Isenberg, 1989; Hoek *et al.* 1997).

An important function of mitochondrial Ca^{2+} signals is the control of energy metabolism. Increases in mitochondrial [Ca^{2+}] ([Ca^{2+}]$_m$), coupled to elevations in [Ca^{2+}]$_c$, participate in activation of the respiratory chain through stimulation of Ca^{2+}-sensitive mitochondrial dehydrogenases, thereby ensuring adequate ATP synthesis (Denton & McCormack, 1980; Hansford, 1981; Duchen, 1992; Pralong *et al.* 1994; Hajnóczky *et al.* 1995; Robb-Gaspers *et al.* 1998; Jouaville *et al.* 1999). Propagation of calcium signals to the mitochondria is also important for apoptotic cell death (Stout *et al.* 1998; Szalai *et al.* 1999). Furthermore, mitochondrial Ca^{2+} transport appears to modulate the spatio-temporal pattern of [Ca^{2+}]$_c$ responses evoked by IP_3, suggesting that mitochondria are also involved in the shaping of [Ca^{2+}]$_c$ signals (Jouaville *et al.* 1995; Budd & Nicholls, 1996; Babcock *et al.* 1997; Hoth *et al.* 1997; Ichas *et al.* 1997; Simpson *et al.* 1997; Landolfi *et al.* 1998; Boitier *et al.* 1999; Hajnóczky *et al.* 1999). However, how much calcium is utilized in mitochondrial signalling during intracellular Ca^{2+} mobilization has not yet been measured.

Our aim was to determine the amount of Ca^{2+} transmitted from SR/ER to the mitochondria during RyR/IP_3R-mediated [Ca^{2+}]$_c$ signals. Since calibration of Ca^{2+} amounts is difficult in intact cells, we established a novel fluorescence Ca^{2+} imaging approach using permeabilized

H9c2 myotubes and RBL-2H3 mast cells, which allowed calibration of Ca^{2+} release and uptake by intracellular organelles by adding known amounts of calcium. In particular, this method was suitable for estimating the relation between SR/ER release and mitochondrial Ca^{2+} uptake. We have already shown that the Ca^{2+} coupling between reticular and mitochondrial Ca^{2+} stores is well preserved in adherent permeabilized cells (Hajnóczky *et al.* 1999; Csordás *et al.* 1999). Furthermore, we found that the morphology of the SR/ER–mitochondrial junctions is retained in permeabilized H9c2 myotubes and RBL-2H3 mast cells. Using these experimental models we show that a large fraction (25–50%) of Ca^{2+} released through RyR and IP_3R can be accumulated by the mitochondria.

METHODS

Cell culture

H9c2 cardiac cells (obtained from American Type Culture Collection, Rockville, MD, USA) were cultured in Dulbecco's modified Eagle's medium supplemented with 10% (v/v) fetal bovine serum, 2 mM glutamine, 100 u ml^{-1} penicillin, 100 μg ml^{-1} streptomycin and 1 mM pyruvate in humidified air (5% CO_2) at 37°C. RBL-2H3 mast cells (kindly provided by Clare Fewtrell) were cultured in Eagle's minimum essential medium supplemented with 20% fetal bovine serum as described previously (Csordás *et al.* 1999). For imaging experiments cells were plated onto poly-D-lysine-coated glass coverslips. H9c2 myoblasts were grown to reach confluency (1 week on average) and subsequently for an additional 4–7 days to allow differentiation to myotubes. Since differentiation of H9c2 myoblasts was associated with the loss of an increasing number of cells from the coverslips and confluent cultures were required to obtain measurable $[Ca^{2+}]$ responses in the bath solution, cultures were used before the differentiation of every cell was completed. As such, mixed populations of multinucleated myotubes and differentiating mononucleated H9c2 cells were imaged in the present studies. The average calculated number of H9c2 and RBL cells on each coverslip was 0.11×10^6 and 1.09×10^6, respectively.

Fluorescence imaging measurements in permeabilized H9c2 and RBL-2H3 cells

Prior to use, the cells were preincubated for 30 min in extracellular medium composed of (mM): 121 NaCl, 5 $NaHCO_3$, 10 Na-Hepes, 4.7 KCl, 1.2 KH_2PO_4, 1.2 $MgSO_4$, 2 $CaCl_2$, 10 glucose and 2% bovine serum albumin (BSA), pH 7.4 at 37°C.

For measurements of $[Ca^{2+}]_m$, the cells were loaded with 5 μM fura-2FF AM or 3 μM rhod-2 AM in the presence of 0.003% (w/v) pluronic acid for 50–70 min. For mitochondrial membrane potential ($\Delta\Psi_m$) measurement, H9c2 cells were loaded with 100 nM tetramethylrhodamine ethyl ester (TMRE) for 15 min. TMRE (10 nM) was also present in the intracellular buffer during the measurements.

Dye-loaded cells were washed with Ca^{2+}-free extracellular buffer composed of (mM): 120 NaCl, 20 Na-Hepes, 5 KCl, 1 KH_2PO_4 and 100 μM EGTA/Tris at pH 7.4. They were then permeabilized by incubation for 5 min with 15 μg ml^{-1} digitonin in intracellular medium composed of (mM): 120 KCl, 10 NaCl, 1 KH_2PO_4, 20 Tris-Hepes at pH 7.2 with 2 mM MgATP, 2 mM succinate and 1 μg ml^{-1} each of antipain, leupeptin and pepstatin. Intracellular medium was passed through a Chelex column to lower the ambient $[Ca^{2+}]$. Medium free $[Ca^{2+}]$ was < 100 nM after Chelex treatment and did not exceed 300–400 nM after addition of ATP, succinate and protease inhibitors. In most of the experiments 20 μM EGTA was also present during permeabilization to maintain low $[Ca^{2+}]$ (< 50 nM) and EGTA-free medium was added after permeabilization. For measurements of perimembrane $[Ca^{2+}]$ ($[Ca^{2+}]_{pm}$) labelling of cells with Calcium Green-C_{18} or fura-C_{18} (1.5–5 μM) was carried out during permeabilization. After permeabilization, the cells were washed into fresh buffer without digitonin and incubated in the imaging chamber, at 35°C.

Changes of the global $[Ca^{2+}]$ in the incubation medium ($[Ca^{2+}]_c$) were measured by the Ca^{2+} tracers fura-2 free acid (FA) (2 μM) and Calcium Green FA (0.25 μM).

Measurements of $[Ca^{2+}]_m$, $[Ca^{2+}]_{pm}$ and $[Ca^{2+}]_c$ were carried out using a multiwavelength beamsplitter/emission filter combination and a high quantum-efficiency cooled CCD camera as described earlier (Hajnóczky & Thomas, 1997; Csordás *et al.* 1999). Excitation at 340 and 380 nm was used for fura-2FF, fura-2 and fura-C_{18}, 490 nm was used for Calcium Green and Calcium Green-C_{18} and 545 nm was used for rhod-2.

To determine the average $[Ca^{2+}]_{pm}$ and $[Ca^{2+}]_m$ signals, mean fluorescence intensities (for rhod-2 and Calcium Green-C_{18}) or ratios (for fura-2FF and fura-C_{18}) were calculated for essentially all individual whole-cell areas in each run after subtraction of the background fluorescence measured at cell-free areas of the field (Figs 3 and 4). To determine changes in $[Ca^{2+}]_c$, fluorescence intensities of fura-2 or Calcium Green dissolved in the incubation medium were taken from the entire field without background subtraction (Figs 3 and 4). The K_d values of 224 nM for fura-2 and 300 nM for Calcium Green were used for calculation of $[Ca^{2+}]_c$.

Confocal imaging of $\Delta\Psi_m$ and two-photon imaging of NAD(P)H were carried out using a BioRad-MRC1024/2P imaging system fitted to an Olympus-IX70 inverted microscope. For confocal imaging a Kr/Ar-ion laser source (568 nm excitation) was used whereas two-photon (2P) imaging was carried out using a pulsed femtosecond laser system (Millennia V/Tsunami, tuned to 720–740 nM, 80 fs pulses) and non-descanned detectors for recording the fluorescence signal.

Experiments were carried out with at least four to five different cell preparations, and 25–100 cells were monitored in each experiment. Traces represent single cell responses unless it is indicated otherwise. The data are shown as means ± S.E.M. Significance of differences from the relevant controls was calculated by Student's *t* test.

Fura-2, fura-2FF, Calcium Green and rhod-2 were obtained from Teflabs (Austin, TX, USA) and Calcium Green-C_{18} and fura-C_{18} were from Molecular Probes (Eugene, OR, USA).

Electron microscopy

Intact and permeabilized cells were fixed in 2% glutaraldehyde, 1% tannic acid, 0.1 M sodium cacodylate at pH 7.4 for 2 h at room temperature. The fixed cells were then carefully detached using a rubber-tipped cell scraper. All samples were washed three times in 0.1 M sodium cacodylate, pH 7.4, and then post-fixed in 1% OsO_4 at room temperature in the same buffer. All samples were then washed three times in distilled water and stained with 1% uranyl acetate and pelleted in 2% agarose. The pellets were dehydrated in graded steps of acetone and embedded into Spurrs resin. Sections (80 nm thick) were cut on a Reichert Ultracut E microtome and stained using uranyl acetate and sodium bismuth. The sections were examined with a Hitachi 7000 scanning transmission electron microscope, and micrographs were obtained using Kodak 4489 film. Electron micrographs are typical of data obtained in two experiments.

Micrographs were collected in all areas of the sections that showed mitochondria and SR/ER. Before measurements, the shape and distribution of organelles were inspected in every micrograph and the organelles visible in more than one section were marked to avoid

double counting of SR/ER–mitochondrial interfaces. The minimum distance between the mitochondrial outer membrane and the nearest SR/ER membrane was measured for all mitochondria included in images.

RESULTS

Ca^{2+} release responses and mitochondrial calcium signals evoked by maximal activation of RyR and IP_3R

First we monitored the Ca^{2+} release evoked by maximal activation of RyR with caffeine (20 mM) in H9c2 myotubes. As shown in Fig. 1*A*, caffeine induced a large increase in perimembrane $[Ca^{2+}]$ ($[Ca^{2+}]_{pm}$) measured with a lipophilic Ca^{2+} probe, fura-C_{18}, anchored to cellular membranes (Fig. 1*A*, i and ii; green to red shift in the overlaid images). The $[Ca^{2+}]_{pm}$ increase was transient as released Ca^{2+} was diluted in the bulk cytosolic medium (Fig. 1*A*, v). Figure 1*A* also shows that the magnitude of the caffeine-induced $[Ca^{2+}]_{pm}$ spike was as large as the $[Ca^{2+}]_{pm}$ elevation caused by addition of 10 μM $CaCl_2$. The mitochondrial $[Ca^{2+}]$ ($[Ca^{2+}]_m$) response elicited by caffeine was measured by rhod-2 compartmentalized in the mitochondria (Hajnóczky *et al.* 1995, 1999; Csordás *et al.* 1999). Figure 1*A* shows that $[Ca^{2+}]_m$ displayed a large increase (iii and iv; shown in red) that was synchronized to the upstroke of the $[Ca^{2+}]_{pm}$ response and was sustained (Fig. 1*A*, v).

Similar measurements of $[Ca^{2+}]_{pm}$ and $[Ca^{2+}]_m$ were also carried out in permeabilized RBL-2H3 mast cells exposed to IP_3. Saturating doses of IP_3 (12.5 μM) elicited a $[Ca^{2+}]_{pm}$ rise as measured by Calcium Green-C_{18} (Fig. 1*B*, i and ii; the fluorescence increase (ΔF) visualized in purple) and the $[Ca^{2+}]_{pm}$ signal was transient (Fig. 1*B*, v). $[Ca^{2+}]_m$ was measured in RBL-2H3 mast cells using fura-2FF as described previously (Csordás *et al.* 1999). All cells in the field showed a $[Ca^{2+}]_m$ rise in association with the $[Ca^{2+}]_{pm}$ spikes (Fig. 1*B*, iii and iv; green to red shift in the overlaid images). The corresponding time course shows a sustained IP_3-induced increase in $[Ca^{2+}]_m$ (Fig. 1*B*, v). Sustained elevations of $[Ca^{2+}]_m$ were not due to saturation of the compartmentalized Ca^{2+} tracers, since addition of 2–5 mM $CaCl_2$ following maximal stimulation of RyR/IP_3R resulted in substantial further increases in $[Ca^{2+}]_m$ (data not shown).

Several mitochondrial dehydrogenases are activated by elevated $[Ca^{2+}]_m$ and this activation can be monitored fluorometrically through changes in pyridine nucleotide redox state (e.g. Duchen, 1992; Pralong *et al.* 1994; Hajnóczky *et al.* 1995). Figure 1*C* shows that the caffeine-induced $[Ca^{2+}]_m$ signal resulted in an increase in NAD(P)H fluorescence in permeabilized H9c2 myotubes, reflecting the Ca^{2+}-dependent dehydrogenase activation. The redox response appeared throughout the cell, apart from the nuclear matrix. These data suggest that regulation of intramitochondrial metabolism by RyR-driven $[Ca^{2+}]_m$ signals is retained in permeabilized H9c2 cells. Measurement of Ca^{2+} signal-dependent NAD(P)H responses was not feasible in RBL-2H3 mast cells owing to the very small NAD(P)H fluorescence in these cells (G. Csordás & G. Hajnóczky, unpublished data).

Close junctions between SR/ER and mitochondrial membranes are thought to be the sites where RyR/IP_3R-mediated Ca^{2+} signals are relayed to the mitochondria (Rizzuto *et al.* 1993, 1998; Csordás *et al.* 1999). We used electron microscopy to study whether the morphology of the contacts between SR/ER and mitochondria is preserved in adherent permeabilized cells. Previous electron microscopy studies have shown close contacts in intact RBL-2H3 cells and cardiomyocytes (Wilson *et al.* 1998; Sharma *et al.* 2000) and preservation of the integrity of intracellular membranes in adherent cardiac cells and hepatocytes permeabilized with low concentrations of digitonin (e.g. Altschuld *et al.* 1985; Renard-Rooney *et al.* 1993). Figure 2 shows electron micrographs of H9c2 cells (*A*) and RBL-2H3 cells (*B*) before (left) and after (right) permeabilization. In intact as well as in permeabilized H9c2 cells two types of SR/ER morphology were observed: polymorph structures with ample intraluminal space mostly in smaller cells (Fig. 2*A*, i and ii) and linear stacks with narrow lumen particularly in the multinucleated myotubes (Fig. 2*A*, iii and iv). Mitochondria appeared as tubular and oval structures in H9c2 cells. Strikingly, most of the mitochondria exhibited close junctions with SR (shown by arrows). Although the intercristal regions of the mitochondria were dilated in permeabilized cells, the close junctions between mitochondria and SR/ER did not appear to be affected by permeabilization of the adherent cells. Less than 100 nm distance was measured between mitochondria and SR/ER for 30 out of 42 mitochondria (71%) and 45 out of 69 mitochondria (65%) in intact and permeabilized H9c2 cells, respectively. The remaining ~30% of mitochondria could also have junctions with SR/ER since we analysed only one section of most of the mitochondria. Furthermore, the distance distribution of the contacts in permeabilized H9c2 cells was not different from that observed in intact cells (Fig. 2*C*), suggesting that permeabilization did not yield an increase of the space between SR/ER and mitochondrial membranes.

In RBL-2H3 cells, the majority of the mitochondria were oval shaped and similar to the H9c2 cells most of the mitochondria appeared in close association with ER (Fig. 2*B*). In intact cells 43 out of 56 mitochondria (77%), and in permeabilized cells 50 out of 66 mitochondria (76%) appeared at less than 100 nm distance from ER and no major difference was found between the distance distribution of the contacts in the two conditions (Fig. 2*C*, right). Interestingly, over 50% of the contacts exhibited less than 24 nm distance between ER and mitochondrial membranes in RBL-2H3 cells, whereas only 30% did in H9c2 cells, suggesting that the local coupling is particularly close in RBL-2H3 cells (Fig. 2*C*). Taken

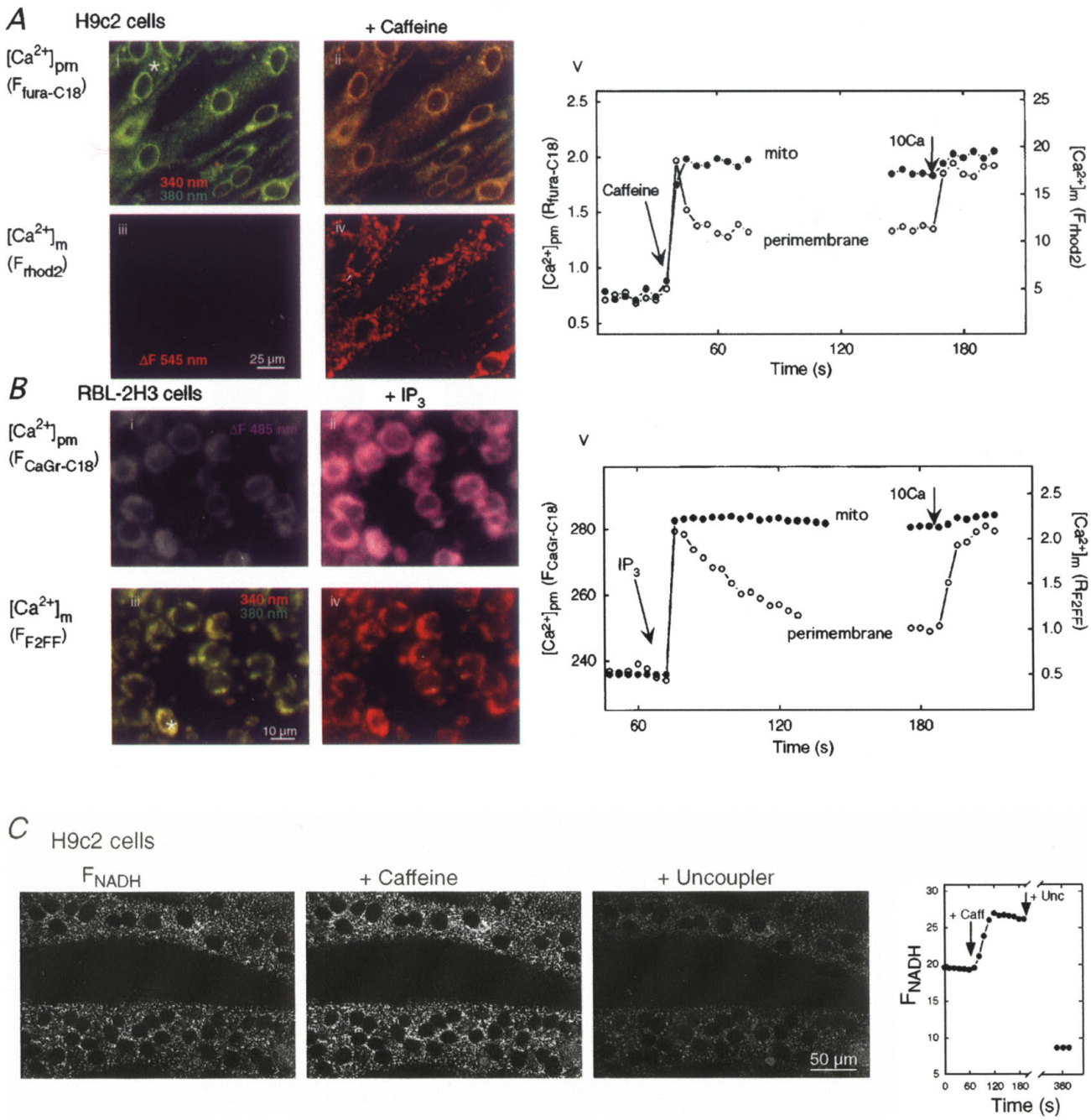

Figure 1. Fluorescence imaging of $[Ca^{2+}]_{pm}$ and $[Ca^{2+}]_m$ and two-photon imaging of NAD(P)H in permeabilized H9c2 myotubes and RBL-2H3 mast cells

A, fluorescence images of H9c2 myotubes before and after caffeine addition (20 mM) using fura-C_{18} (i and ii) and compartmentalized rhod-2 (iii and iv) to obtain simultaneous measurements of $[Ca^{2+}]_{pm}$ and $[Ca^{2+}]_m$. *B*, fluorescence images of RBL-2H3 mast cells before and after stimulation with IP_3 (12.5 μM) using Calcium Green-C_{18} (i and ii) and compartmentalized fura-2FF (iii and iv). The corresponding time courses of $[Ca^{2+}]_{pm}$ and $[Ca^{2+}]_m$ during RyR/IP_3R stimulation and Ca^{2+} (10μM $CaCl_2$) addition are shown in v. Fluorescence signals were calculated for the total extranuclear area of the cells marked with an asterisk. F_{rhod2} and $F_{Calcium\ Green\text{-}C18}$ are shown as fluorescence arbitrary units (f.a.u.). Fura-C_{18} (*A*, i and ii) and fura-2FF (*B*, iii and iv) fluorescence are shown as overlays of images collected at 340 nm (red, increases from Ca^{2+}) and 380 nm excitation (green, decreases from Ca^{2+}). Rhod-2 (*A*, iii and iv) and Calcium Green-C_{18} (*B*, i and ii) fluorescence is shown in grey-scale and the fluorescence changes (ΔF) are visualized in red and purple, respectively. *C*, two-photon imaging of the NAD(P)H response to caffeine in permeabilized H9c2 myotubes. The grey images show the NAD(P)H fluorescence in two multinucleated permeabilized myotubes before stimulation (left), after stimulation with caffeine (20 mM, middle) and after treatment with the uncoupler carbonyl cyanide *p*-(trifluoromethoxy)phenylhydrazone (FCCP; 5 μg ml^{-1}, right). The uncoupler was used to stimulate mitochondrial oxidation. Because of the absence of mitochondria in the nuclear matrix, the nuclei are visible as dark circles. Time course of the $F_{NAD(P)H}$ signal (in f.a.u.) was calculated for the total extranuclear area of the cell shown in the upper part of the images.

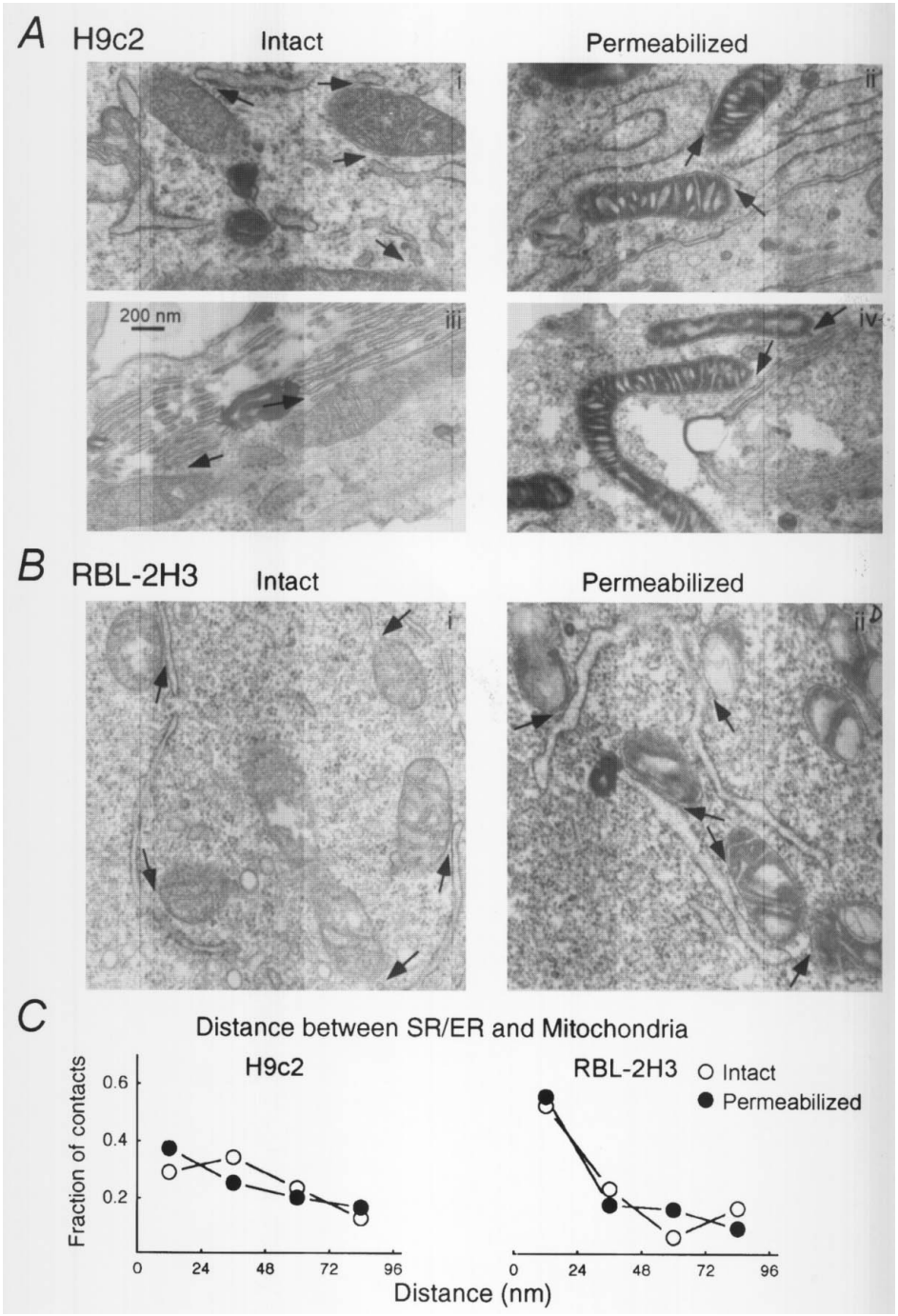

Figure 2. Morphology of the junctions between SR/ER and mitochondria in intact and permeabilized H9c2 and RBL-2H3 cells

Electron micrographs of H9c2 myotubes (*A*) and RBL-2H3 mast cells (*B*). In each case intact cells are shown in the left and permeabilized cells are shown in the right panels. Two pairs of micrographs of H9c2 cells are shown to illustrate the two typical patterns of ER morphology observed in these cells. Arrows indicate the close junctions between SR/ER and mitochondria. *C*, distance distribution of the junctions between SR/ER and mitochondria. Close appositions of SR/ER and mitochondrial membranes (< 100 nm distance) were sorted into four groups, < 24, 24–48, 48–72, 72–96 nm distance, and the number of contacts in each group was normalized to the total number of contacts (H9c2: intact, 42 contacts; permeabilized, 67 contacts; RBL-2H3: intact, 62 contacts; permeabilized, 64 contacts).

together, these electron microscopy data demonstrated preservation of the morphology of the contacts between SR/ER and mitochondria in permeabilized H9c2 and RBL-2H3 cells. Although the intramitochondrial morphology was affected by permeabilization, the RyR/IP_3R-mediated $[Ca^{2+}]_m$ and NAD(P)H signals suggest that mitochondrial calcium regulation was retained in the permeabilized cells.

In summary, the rapid and large increases of $[Ca^{2+}]_m$ show the efficient propagation of RyR- and IP_3R-mediated Ca^{2+} signals to the mitochondria in permeabilized H9c2 myotubes and RBL-2H3 mast cells. Preservation of the close contacts between SR/ER and mitochondria in permeabilized H9c2 and RBL-2H3 cells provides the basis of local calcium signal transmission. Furthermore, the RyR-dependent NAD(P)H responses show that propagation of calcium signals to the mitochondria results in activation of the mitochondrial effectors in permeabilized cells. Also the rise in $[Ca^{2+}]_m$ following maximal stimulation of RyR/IP_3R was sustained in both cell types suggesting that mitochondria retained the accumulated Ca^{2+}. As such, the amount of Ca^{2+} releasable from the mitochondria during the sustained phase of $[Ca^{2+}]_m$ signals can be used as a measure of the Ca^{2+} taken up during RyR/IP_3R activation.

Measurements of global $[Ca^{2+}]$ in the cytosolic compartment

To determine the amount of Ca^{2+} discharged from the mitochondria we designed an approach to measure released Ca^{2+} in the cytosolic buffer. As shown in Fig. 1, Ca^{2+} release from the stores yielded transient elevations of $[Ca^{2+}]$ to the micromolar range in the vicinity of membranes. By contrast, Ca^{2+} release was anticipated to yield small changes of global $[Ca^{2+}]_c$, owing to the cell permeabilization-induced expansion of the cytosolic space. To increase the changes in global $[Ca^{2+}]$ we used confluent cultures. Under these conditions 170 ± 3 ($n = 4$) or 340 ± 15 μg protein ($n = 2$) of permeabilized H9c2 myotubes or RBL-2H3 mast cells was used. Since the size of the SR/ER Ca^{2+} store was reported to be in the range of 2 to > 20 nmol (mg protein)$^{-1}$ in permeabilized cells (e.g. Altschuld *et al.* 1985; Biden *et al.* 1986; Kindman & Meyer, 1993), we estimated that caffeine or IP_3 may release at least 0.5 nmol Ca^{2+} from the confluent

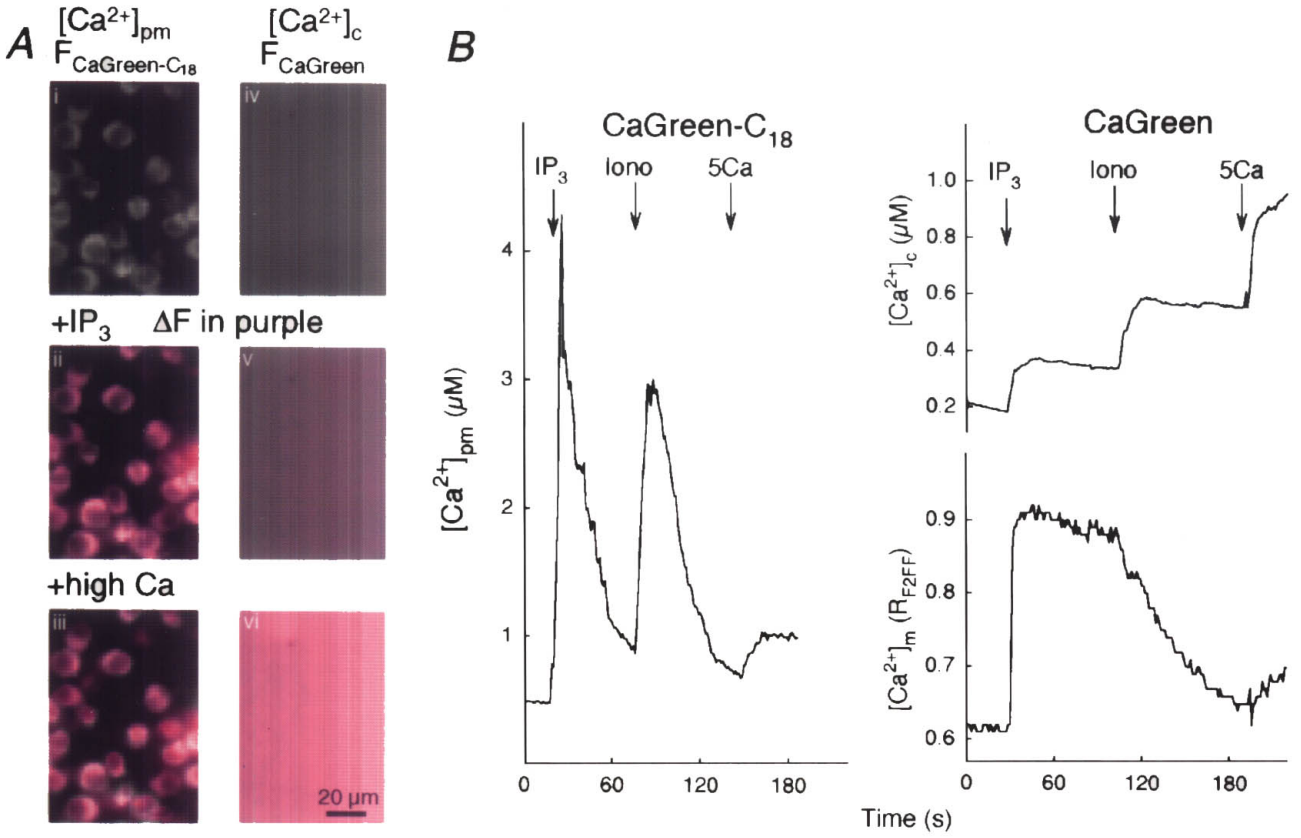

Figure 3. Changes of perimembrane and global $[Ca^{2+}]_c$ during Ca^{2+} mobilization

A, i and iv, grey-scale images show the fluorescence of Calcium Green-C_{18} attached to permeabilized RBL-2H3 mast cells (left) and Calcium Green added to the medium (right). Increases of the fluorescence (ΔF) evoked by IP_3-induced Ca^{2+} release (ii and v) and a saturating dose of $CaCl_2$ (1.5 mM, high calcium, iii and vi) are shown in purple. *B*, time course of the $[Ca^{2+}]_{pm}$ responses evoked by IP_3 (12.5 μM), ionomycin (Iono, 10 μM) and Ca^{2+} (5 μM, 5Ca) are shown on the left. Time courses of $[Ca^{2+}]_c$ recorded simultaneously with $[Ca^{2+}]_m$ are shown on the right.

cultures to the 1 ml volume of buffer in the imaging chamber. We also postulated that a relatively low Ca^{2+} binding ratio in the cytosolic buffer may partially compensate for the increased cytosolic volume resulting from cell permeabilization. To establish a calibration for $[Ca^{2+}]$ in the cytosolic buffer taking into account Ca^{2+} buffering we added known amounts of Ca^{2+} to give a total Ca^{2+} load of 5 μM, and calibrated the effective change in $[Ca^{2+}]_c$ achieved using fura-2. The $[Ca^{2+}]_c$ increase was 680 ± 23 nM ($n = 30$), suggesting that the Ca^{2+} binding ratio is approximately 6. Although cytosolic Ca^{2+} binding ratios have not been reported for H9c2 myotubes or RBL-2H3 cells, in cardiac muscle the global cytosolic Ca^{2+} binding ratio is between 50 and 128 at submicromolar $[Ca^{2+}]$ (for review see Neher, 1995). Thus, a weaker Ca^{2+} buffering in the cytosolic buffer may facilitate intracellular Ca^{2+} mobilization to evoke measurable increases of $[Ca^{2+}]$ in the expanded cytosolic space. Since propagation of RyR/IP_3R-mediated Ca^{2+} signals to the mitochondria is likely to occur at the SR/ER mitochondrial junctions and the ability of Ca^{2+} buffers to move between the junctions and the global cytosolic space is not known, it is not clear whether dilution of the cytosol also affects Ca^{2+} signalling to the mitochondria. One clue to this point is that propagation of IP_3R-mediated Ca^{2+} signals to the mitochondria is relatively insensitive to increases in global $[Ca^{2+}]_c$ buffering in RBL-2H3 mast cells (Csordás *et al.* 1999). Taken together, on the basis of these data we predicted that intracellular Ca^{2+} mobilization from confluent cell cultures yields a measurable increase in the bulk $[Ca^{2+}]_c$.

First, parallel measurements of $[Ca^{2+}]_{pm}$ and $[Ca^{2+}]_c$ were carried out in permeabilized RBL-2H3 mast cells using Calcium Green-C_{18} and Calcium Green FA, respectively. Using Calcium Green-C_{18} the IP_3-induced $[Ca^{2+}]$ elevation appeared as a large fluorescence increase over the cells (Fig. 3*A*, ii; ΔF is shown in purple), whereas using Calcium Green a small fluorescence increase was measured all over the image (Fig. 3*A*, v). Incubation with Calcium Green-C_{18} and Calcium Green was set so that the maximal fluorescence increase evoked by $CaCl_2$ (1.5 mM) was similar using these two Ca^{2+} tracers (Fig. 3*A*, iii and vi). As Calcium Green-C_{18} was attached to cellular membranes the fluorescence increase caused by saturating $[Ca^{2+}]$ was visible above the cells, whereas the $[Ca^{2+}]$ rise detected by Calcium Green was homogeneous. In addition to the difference in magnitude and spatial pattern between IP_3-induced $[Ca^{2+}]_{pm}$ and $[Ca^{2+}]_c$ responses, the time courses revealed that IP_3 and Ca^{2+} ionophore (ionomycin)-dependent $[Ca^{2+}]_{pm}$ signals appeared as spikes, whereas the $[Ca^{2+}]_c$ signals were sustained (Fig. 3*B*). It is noteworthy that the calibrating Ca^{2+} pulse ($CaCl_2$ 5 μM) added after ionomycin caused very similar increases in $[Ca^{2+}]_{pm}$ and $[Ca^{2+}]_c$ (Fig. 3*B* left *vs.* upper right) underscoring that the difference in the $[Ca^{2+}]$ change evoked by IP_3 was not due to differences in the sensitivity of the two probes to Ca^{2+}. Simultaneous measurements of $[Ca^{2+}]_c$ and $[Ca^{2+}]_{pm}$ carried out using Calcium Green and compartmentalized fura-2FF show that the IP_3-induced $[Ca^{2+}]_c$ signal was associated with a rapid and large $[Ca^{2+}]_m$ rise (right panel). Addition of ionomycin caused a decay of $[Ca^{2+}]_m$ and simultaneous rise in $[Ca^{2+}]_c$. $[Ca^{2+}]_c$ increases were calibrated with Ca^{2+} pulses added at the end of each run. In permeabilized H9c2 myotubes $[Ca^{2+}]_c$ and $[Ca^{2+}]_m$ were measured using fura-2FA dissolved in the incubation medium and compartmentalized rhod-2, respectively. The pattern of $[Ca^{2+}]_c$ signals evoked by intracellular Ca^{2+} mobilization in H9c2 myotubes was essentially the same as it was in RBL-2H3 mast cells (Fig. 4, see below).

Collectively, these data demonstrated that Ca^{2+} release in permeabilized H9c2 myotubes and RBL-2H3 mast cells can be measured by monitoring global $[Ca^{2+}]_c$. The sustained temporal pattern of the $[Ca^{2+}]_c$ changes and simple calibration of the $[Ca^{2+}]_c$ signals give an opportunity to determine the amount of Ca^{2+} mobilized from different intracellular stores.

Quantification of mitochondrial Ca^{2+} uptake

Figure 4*A* shows $[Ca^{2+}]_c$ and $[Ca^{2+}]_m$ signals during mobilization of the SR and mitochondrial Ca^{2+} stores in H9c2 myotubes. Maximal activation of the RyR with caffeine yielded rapid and prolonged elevations in $[Ca^{2+}]_c$ and $[Ca^{2+}]_m$ (top and middle). It is assumed that the initial rise of $[Ca^{2+}]_c$ over the plateau level was due to the fact that the image was focused on the cells and so a fraction of the Ca^{2+} tracer sensed the initial $[Ca^{2+}]$ burst in the vicinity of the Ca^{2+} stores. The amount of Ca^{2+} released by caffeine was determined using the plateau level (marked by dashed lines). To establish complete depletion of the reticular stores we added Tg, which caused an increase in $[Ca^{2+}]_c$, whereas $[Ca^{2+}]_m$ remained unchanged (top and middle). Then a supramaximal dose of ionomycin (10 μM) was added to release Ca^{2+} from all the remaining non-acidic membrane compartments. After complete depletion of the reticular stores, Ca^{2+} released by ionomycin can be considered to be of mitochondrial origin in most cell types (Hoth *et al.* 1997). In support of this point, the ionomycin-induced $[Ca^{2+}]_c$ rise was associated with a decrease in $[Ca^{2+}]_m$ (upper right), and pretreatment with uncoupler (FCCP/oligomycin 5 μg ml^{-1} each) that dissipates $\Delta\Psi_m$ (Fig. 4*B*, $\Delta\Psi_m$ was measured using TMRE), the driving force for mitochondrial Ca^{2+} accumulation, markedly reduced ionomycin-induced Ca^{2+} release after complete discharge of the SR by caffeine + Tg (Fig. 4*A*; upper left *vs.* lower left; statistics are shown in Fig. 5*A*). Alternatively, uncoupler was used to release Ca^{2+} from the mitochondria after caffeine-induced Ca^{2+} mobilization from the SR in H9c2 cells (Fig. 4*A*, middle). Addition of uncoupler after ionomycin or vice versa did not cause a significant decrease in $[Ca^{2+}]_m$ (not shown). Furthermore, Fig. 4*A* shows that uncoupler eliminated propagation of the $[Ca^{2+}]_c$ signal to the mitochondria (lower right).

To calculate the amount of Ca^{2+} released from SR by caffeine + Tg and from mitochondria by ionomycin or uncoupler, the $[Ca^{2+}]_c$ rises were calibrated with application of known amounts of Ca^{2+}. In our experiments the relation between the $\Delta[Ca^{2+}]_c$ and amounts of Ca^{2+} added was linear in the range of changes caused by mobilization of intracellular stores, and thus we used the following equation to express Ca^{2+}

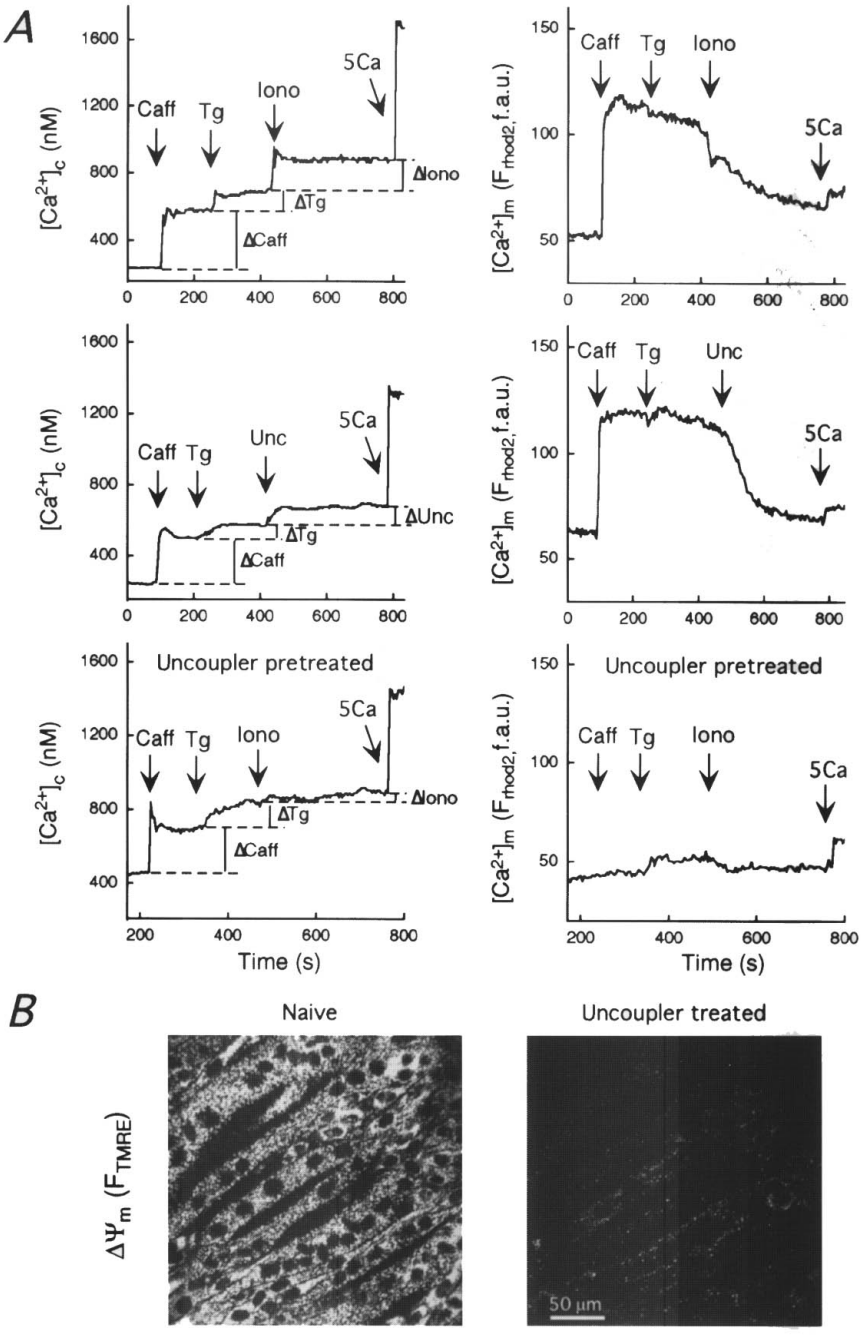

Figure 4. Effect of Ca^{2+} mobilization from SR on $[Ca^{2+}]_c$, $[Ca^{2+}]_m$ and $\Delta\Psi_m$

A, time courses of $[Ca^{2+}]_m$ and $[Ca^{2+}]_c$ recorded in permeabilized H9c2 myotubes exposed to caffeine (Caff, 20 mM), thapsigargin (Tg, 2 μM), ionomycin (Iono, 10 μM, top) or uncoupler (Unc: FCCP/oligomycin, 5 μg ml^{-1} each, middle). The experiment in the top panel was repeated on uncoupler-pretreated cells (lower panel). $[Ca^{2+}]_m$ and $[Ca^{2+}]_c$ were measured using compartmentalized rhod-2 and fura-2FA (2 μM) dissolved in the incubation medium, respectively. For calculations of Ca^{2+} amounts a calibrating pulse of Ca^{2+} ($CaCl_2$, 5 μM) was applied at the end of each run. *B*, confocal images of TMRE-loaded permeabilized H9c2 myotubes before (left) and after (right) exposure to uncoupler. The fluorescence intensity of TMRE reflecting $\Delta\Psi_m$ is shown using grey-scale.

uptake/release in terms of nanomoles of Ca^{2+}:

$$\Delta Ca^{2+}{}_x = \Delta[Ca^{2+}]_{cx} \times \Delta Ca^{2+}{}_{cal} / \Delta[Ca^{2+}]_{ccal},$$

where $\Delta Ca^{2+}{}_x$ (nmol) is the amount of Ca^{2+} to be determined, $\Delta[Ca^{2+}]_{cx}$ is the corresponding change in the $[Ca^{2+}]_c$, $\Delta Ca^{2+}{}_{cal}$ is the amount of Ca^{2+} used for calibration (nmol) and $\Delta[Ca^{2+}]_{ccal}$ is the increase in $[Ca^{2+}]_c$ caused by the calibrating Ca^{2+} pulse.

Figure 5 shows the fractions of Ca^{2+} released by the different manipulations in H9c2 myotubes (Fig. 5*A*) and in RBL-2H3 mast cells (Fig. 5*B*). The amount of Ca^{2+} released by caffeine + Tg was 3.32 ± 0.17 nmol ($n = 18$; 20 nmol (mg protein)$^{-1}$) in naive and 4.13 ± 0.40 nmol ($n = 7$) in uncoupler-pretreated H9c2 myotubes, respectively. As uncoupler prevents mitochondrial Ca^{2+} uptake (e.g. Fig. 4) the uncoupler-dependent increase in the $[Ca^{2+}]_c$ response elicited by caffeine + Tg ($P < 0.05$) was used as a measure of mitochondrial Ca^{2+} accumulation.

The uncoupler-dependent increase in Ca^{2+} release evoked by caffeine + Tg was associated with a decrease in the residual Ca^{2+} released by subsequent addition of ionomycin (Fig. 5*A*; 1.15 ± 0.12 *vs.* 0.56 ± 0.06 nmol Ca^{2+} in naive and uncoupler-pretreated cells, $n = 13$ and 7, $P < 0.01$). The uncoupler-dependent decrease in ionomycin-induced Ca^{2+} release was also used as a measure of mitochondrial sequestration of Ca^{2+} mobilized from the SR, though uncoupler pretreatment could also attenuate ionomycin-induced Ca^{2+} release by mobilization of Ca^{2+} that had been present in the mitochondria prior to Ca^{2+} release. Thus, we also measured the amount of Ca^{2+} released by uncoupler added before and after caffeine + Tg-induced Ca^{2+} release. Mitochondrial uptake of released Ca^{2+} was expected to increase the uncoupler-sensitive store. Uncoupler-induced Ca^{2+} release was larger after mobilization of the SR store and the increase was similar to the change of the ionomycin-induced release (0.89 ± 0.11 *vs.* 0.39 ± 0.07 nmol in caffeine + Tg-treated and in naive cells, $n = 5$, $P < 0.01$). Based on these measurements the fraction of Ca^{2+} taken up by the mitochondria during Ca^{2+} mobilization from the SR was ~15% (19.2, 14.3 and 12.1% as calculated from the changes in the caffeine + Tg, ionomycin and uncoupler-induced $[Ca^{2+}]_c$ responses, respectively).

Importantly, caffeine added by itself mobilized 70–80% of the Tg-sensitive store in H9c2 myotubes and Tg-induced release of the residual Ca^{2+} was poorly transmitted to the mitochondria (Fig. 4*A*). Figure 5*A* shows that the mitochondrial Ca^{2+} uptake calculated from the uncoupler-dependent increase in the caffeine-induced $[Ca^{2+}]_c$ response was as large as it was when Tg was also added (0.85 *vs.* 0.79 nmol). From the uncoupler-dependent increment of the caffeine-induced $[Ca^{2+}]_c$ response, mitochondria were calculated to accumulate 26% of the mobilized Ca^{2+}. Taken together, these results demonstrated that a large fraction of the Ca^{2+} released via RyR (26%) can be taken up by the mitochondria. It remains to be determined whether the caffeine-insensitive component of the SR/ER Ca^{2+} store (20–30%) displays local Ca^{2+} communication with mitochondria. Discharge of the caffeine-insensitive store with Tg failed to support mitochondrial Ca^{2+} uptake in the present experiments but Tg has also been shown to mobilize RyR/IP_3R-sensitive stores with little mitochondrial Ca^{2+} accumulation in permeabilized RBL-2H3 cells, suggesting that coordinated activation of the release sites is required for optimal activation of mitochondrial Ca^{2+} uptake sites (Csordás *et al.* 1999).

In naive RBL-2H3 mast cells IP_3 + Tg-induced Ca^{2+} release to the cytosolic buffer was 1.43 ± 0.14 nmol ($n = 8$; 4.2 nmol (mg protein)$^{-1}$) whereas in uncoupler-pretreated cells 1.8 ± 0.2 nmol ($n = 11$) was liberated. The size of the SR/ER store is smaller in RBL-2H3 cells than in H9c2 myotubes (4.2 *vs.* 20 nmol (mg protein)$^{-1}$), consistent with the relatively low density of ER shown by the electron micrographs of RBL-2H3 cells (Fig. 2). It is noteworthy that IP_3 releases the entire Tg-sensitive Ca^{2+} store in RBL-2H3 mast cells (e.g. Csordás *et al.* 1999).

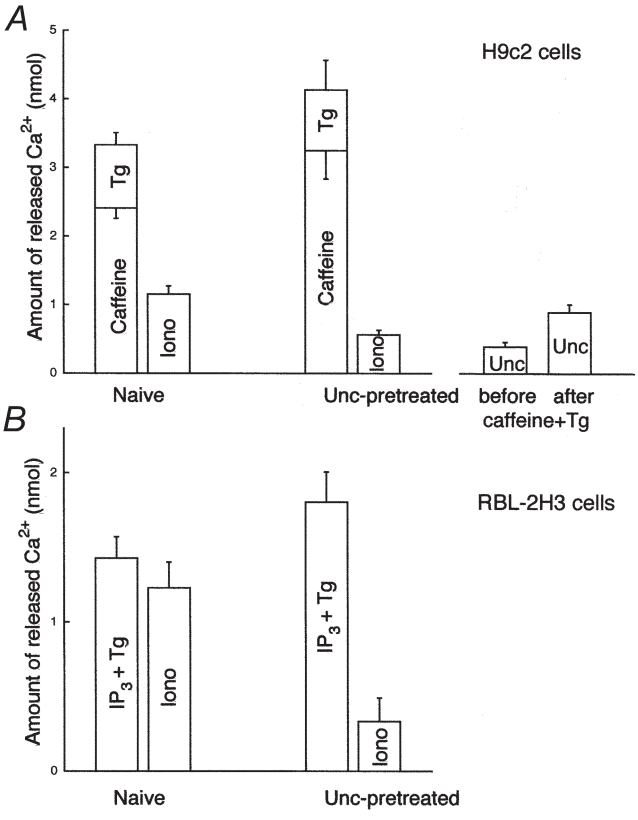

Figure 5. Quantification of Ca^{2+} redistribution between intracellular Ca^{2+} stores during Ca^{2+} mobilization

Amounts of Ca^{2+} released upon addition of caffeine (20 mM), Tg (2 μM) or IP_3 + Tg (12.5 μM IP_3, 2 μM Tg), and ionomycin (Iono,10 μM) in naive and uncoupler (Unc, FCCP + oligomycin)-pretreated H9c2 myotubes (*A*) and RBL-2H3 mast cells (*B*).

Similar to H9c2 myotubes, in uncoupler-pretreated RBL-2H3 mast cells, the augmented IP_3 + Tg-induced Ca^{2+} release was followed by a small ionomycin-induced Ca^{2+} release (Fig. 5*B*; 1.23 ± 0.17 *vs.* 0.33 ± 0.16 nmol Ca^{2+} in naive and uncoupler-pretreated cells, $n = 11$ and 8, $P < 0.01$). Thus the mitochondrial Ca^{2+} uptake calculated from the difference in magnitude of the IP_3 + Tg-induced $[Ca^{2+}]_c$ responses recorded in naive and uncoupler-pretreated cells was 20% of the total release, whereas it was estimated to be 50% using the uncoupler-dependent change in ionomycin-induced release responses in RBL-2H3 mast cells. In mast cells secretory granules represent an uncoupler-sensitive and ionomycin-insensitive Ca^{2+} store. If Ca^{2+} is released from secretory granules during IP_3-induced Ca^{2+} mobilization as reported (e.g. Nguyen *et al.* 1998), calculations based on the uncoupler-dependent change in the effect of IP_3 + Tg may lead to underestimation of mitochondrial Ca^{2+} uptake. Our observation that most of the contacts between ER and mitochondria are very close in RBL-2H3 cells (Fig. 2) is also in support of a particularly effective mitochondrial Ca^{2+} load during IP_3-induced Ca^{2+} release.

DISCUSSION

In the present study we have described a fluorescence imaging method that can be used for quantitative measurement of RyR- or IP_3R-mediated SR/ER Ca^{2+} release and mitochondrial Ca^{2+} uptake in permeabilized cells. In essence, we established measurements of Ca^{2+} mobilized from the intracellular stores of permeabilized adherent cells to the cytosolic buffer. Although cell permeabilization would not necessarily be expected to leave unaffected Ca^{2+} delivery to the mitochondria, evidence is emerging that calcium signal transmission to the mitochondria is controlled by a local $[Ca^{2+}]_c$ regulation between RyR/IP_3R and mitochondrial Ca^{2+} uptake sites and that this local $[Ca^{2+}]_c$ regulation is preserved in carefully permeabilized adherent cells (Rizzuto *et al.* 1993, 1998; Csordás *et al.* 1999; Hajnóczky *et al.* 1999). This idea is further supported by the present electron microscopy data demonstrating preservation of the morphology of the SR/ER–mitochondrial junctions in permeabilized cells and also by the imaging studies showing large RyR/IP_3R-driven mitochondrial matrix $[Ca^{2+}]$ and NAD(P)H signals in individual permeabilized cells. Importantly, the experimental protocol used for cell permeabilization and calcium imaging was also designed to avoid changes in the loading state of Ca^{2+} stores. Thus, the calcium imaging approach we used can provide quantitative information relevant for the physiological redistribution of Ca^{2+} between SR/ER and mitochondria during RyR/IP_3R-mediated Ca^{2+} mobilization.

We have used a mode of stimulation in which synchronized activation of the release sites occurs in all permeabilized cells present in the incubation chamber. Also, we used relatively weak Ca^{2+} buffering in the cytosolic medium. These conditions have allowed us to monitor SR/ER and mitochondrial Ca^{2+} transport by measuring $[Ca^{2+}]_c$ in the bulk bathing medium. Importantly, it has been demonstrated previously that propagation of RyR/IP_3R-mediated Ca^{2+} signals to the mitochondria is relatively insensitive to changes in global $[Ca^{2+}]_c$ buffering (Rizzuto *et al.* 1993; Csordás *et al.* 1999; Sharma *et al.* 2000; Szalai *et al.* 2000). This suggests that dilution of the cytosol fails to affect the Ca^{2+} buffering component which is important in the local Ca^{2+} transfer between SR/ER release sites and mitochondrial Ca^{2+} uptake sites. Furthermore, a fundamental feature of intracellular calcium signalling is that synchronized activation of IP_3R and RyR establishes $[Ca^{2+}]_c$ oscillations, the frequency of which is controlled by the intensity of stimulation. Mitochondrial Ca^{2+} uptake seems to be associated with the rapid rise of $[Ca^{2+}]_c$ responses and so loading of mitochondria by Ca^{2+} released during calcium spikes in intact cells may be as large as we calculated using permeabilized cells exposed to maximal doses of caffeine or IP_3.

The most important finding of this study is that a large fraction of the Ca^{2+} released via RyR or IP_3R can be taken up by the mitochondria. In carefully permeabilized adherent H9c2 myotubes, 26% of Ca^{2+} released via RyR was delivered to the mitochondria, whereas in RBL-2H3 cells 50% of Ca^{2+} released through IP_3R was taken up by the mitochondria. As the mitochondrial matrix volume represents a relatively small fraction of the total cytosolic volume, mitochondrial accumulation of 25–50% of Ca^{2+} released to the cytosol allows elevation of $[Ca^{2+}]_m$ well above the $[Ca^{2+}]_c$ level. Elevation of $[Ca^{2+}]_m$ controls the function of mitochondrial effectors such as Ca^{2+}-sensitive dehydrogenases and the permeability transition pore. Another important conclusion of our study is concerned with the spatial distribution of Ca^{2+} release through the SR/ER membrane. Since calcium signal transmission from SR/ER to the mitochondria depends on a local control between RyR/IP_3 and mitochondrial Ca^{2+} uptake sites and only subregions of the SR/ER surface are close to the mitochondia (e.g. Rizzuto *et al.* 1998; see also Fig. 2), delivery of 25–50% of released Ca^{2+} to the mitochondria may occur only if Ca^{2+} release is concentrated at SR/ER subdomains facing mitochondria. Remarkably, this functional organization allows mitochondria to contribute to the control over activation and deactivation of RyR/IP_3R, to the shaping of global $[Ca^{2+}]_c$ signals and also to the recharging of reticular Ca^{2+} stores. Taken together, the local transfer of substantial amounts of Ca^{2+} to the mitochondria demonstrated in the present study is important for the multiple physiological roles of mitochondrial calcium signalling in the regulation of extra- and intramitochondrial Ca^{2+}-dependent effector mechanisms.

Altschuld, R. A., Wenger, W. C., Lamka, K. G., Kindig, O. R., Capen, C. C., Mizuhira, V., Vander Heide, R. S. & Brierley, G. P. (1985). Structural and functional properties of adult rat heart myocytes lysed with digitonin. *Journal of Biological Chemistry* **260**, 14325–14334.

Babcock, D. F., Herrington, J., Goodwin, P. C., Park, Y. B. & Hille, B. (1997). Mitochondrial participation in the intracellular Ca^{2+} network. *Journal of Cell Biology* **136**, 833–844.

Babcock, D. F. & Hille, B. (1998). Mitochondrial oversight of cellular Ca^{2+} signaling. *Current Opinion in Neurobiology* **8**, 398–404.

Biden, T. J., Wollheim, C. B. & Schlegel, W. (1986). Inositol 1,4,5-trisphosphate and intracellular Ca^{2+} homeostasis in clonal pituitary cells (GH3). Translocation of Ca^{2+} into mitochondria from a functionally discrete portion of the nonmitochondrial store. *Journal of Biological Chemistry* **261**, 7223–7229.

Boitier, E., Rea, R. & Duchen, M. R. (1999). Mitochondria exert a negative feedback on the propagation of intracellular Ca^{2+} waves in rat cortical astrocytes. *Journal of Cell Biology* **145**, 795–808.

Budd, S. L. & Nicholls, D. G. (1996). Mitochondria, calcium regulation, and acute glutamate excitotoxicity in cultured cerebellar granule cells. *Journal of Neurochemistry* **67**, 2282–2291.

Chacon, E., Ohata, H., Harper, I. S., Trollinger, D. R., Herman, B. & Lemasters, J. J. (1996). Mitochondrial free calcium transients during excitation-contraction coupling in rabbit cardiac myocytes. *FEBS Letters* **382**, 31–36.

Csordás, G., Thomas, A. P. & Hajnóczky, G. (1999). Quasi-synaptic calcium signal transmission between endoplasmic reticulum and mitochondria. *EMBO Journal* **18**, 96–108.

Denton, R. M. & McCormack, J. G. (1980). On the role of the calcium transport cycle in heart and other mammalian mitochondria. *FEBS Letters* **119**, 1–8.

Drummond, R. M. & Tuft, R. A. (1999). Release of Ca^{2+} from the sarcoplasmic reticulum increases mitochondrial [Ca^{2+}] in rat pulmonary artery smooth muscle cells. *Journal of Physiology* **516**, 139–147.

Duchen, M. R. (1992). Ca^{2+}-dependent changes in the mitochondrial energetics in single dissociated mouse sensory neurons. *Biochemical Journal* **283**, 41–50.

Duchen, M. R. (1999). Contributions of mitochondria to animal physiology: from homeostatic sensor to calcium signalling and cell death. *Journal of Physiology* **516**, 1–17.

Hajnóczky, G., Csordás, G., Krishnamurthy, R. & Szalai, G. (2000). Mitochondrial calcium signaling driven by the IP_3 receptor. *Journal of Bioenergetics and Biomembranes* **32**, 15–25.

Hajnóczky, G., Hager, R. & Thomas, A. P. (1999). Mitochondria suppress local feedback activation of inositol 1,4,5-trisphosphate receptors by Ca^{2+}. *Journal of Biological Chemistry* **274**, 14157–14162.

Hajnóczky, G., Robb-Gaspers, L. D., Seitz, M. B. & Thomas, A. P. (1995). Decoding of cytosolic calcium oscillations in the mitochondria. *Cell* **82**, 415–424.

Hajnóczky, G. & Thomas, A. P. (1997). Minimal requirements for calcium oscillations driven by the IP_3 receptor. *EMBO Journal* **16**, 3533–3543.

Hansford, R. G. (1981). Effect of micromolar concentrations of free Ca^{2+} ions on pyruvate dehydrogenase interconversion in intact rat heart mitochondria. *Biochemical Journal* **194**, 721–732.

Hoek, J. B., Walajtys-Rode, E. & Wang, X. (1997). Hormonal stimulation, mitochondrial Ca^{2+} accumulation, and the control of the mitochondrial permeability transition in intact hepatocytes. *Molecular and Cellular Biochemistry* **174**, 173–179.

Hoth, M., Fanger, C. M. & Lewis, R. S. (1997). Mitochondrial regulation of store-operated calcium signaling in T lymphocytes. *Journal of Cell Biology* **137**, 633–648.

Hüser, J., Blatter, L. A. & Sheu, S. S. (2000). Mitochondrial calcium in heart cells: beat-to-beat oscillations or slow integration of cytosolic transients? *Journal of Bioenergetics and Biomembranes* **32**, 27–33.

Ichas, F., Jouaville, L. S. & Mazat, J. P. (1997). Mitochondria are excitable organelles capable of generating and conveying electrical and calcium signals. *Cell* **89**, 1145–1153.

Jouaville, L. S., Ichas, F., Holmuhamedov, E. L., Camacho, P. & Lechleiter, J. D. (1995). Synchronization of calcium waves by mitochondrial substrates in *Xenopus laevis* oocytes. *Nature* **377**, 438–441.

Jouaville, L. S., Ichas, F. & Mazat, J. P. (1998). Modulation of cell calcium signals by mitochondria. *Molecular and Cellular Biochemistry* **184**, 371–376.

Jouaville, L. S., Pinton, P., Bastianutto, C., Rutter, G. A. & Rizzuto, R. (1999). Regulation of mitochondrial ATP synthesis by calcium: Evidence for a long-term metabolic priming. *Proceedings of the National Academy of Sciences of the USA* **96**, 13807–13812.

Kindman, L. A. & Meyer, T. (1993). Use of intracellular Ca^{2+} stores from rat basophilic leukemia cells to study the molecular mechanism leading to quantal Ca^{2+} release by inositol 1,4,5-trisphosphate. *Biochemistry* **32**, 1270–1277.

Landolfi, B., Curci, S., Debellis, L., Pozzan, T. & Hofer, A. M. (1998). Ca^{2+} homeostasis in the agonist-sensitive internal store: functional interactions between mitochondria and the ER measured in situ in intact cells. *Journal of Cell Biology* **142**, 1235–1243.

Neher, E. (1995). The use of fura-2 for estimating Ca buffers and Ca fluxes. *Neuropharmacology* **34**, 1423–1442.

Nguyen, T., Chin, W.C. & Verdugo, P. (1998). Role of Ca^{2+}/K^+ ion exchange in intracellular storage and release of Ca^{2+}. *Nature* **395**, 908–912.

Pralong, W. F., Spät, A. & Wollheim, C. B. (1994). Dynamic pacing of cell metabolism by intracellular Ca^{2+} transients. *Journal of Biological Chemistry* **269**, 27310–27314.

Rizzuto, R., Brini, M., Murgia, M. & Pozzan, T. (1993). Microdomains with high Ca^{2+} close to IP_3-sensitive channels that are sensed by neighboring mitochondria. *Science* **262**, 744–747.

Rizzuto, R., Pinton, P., Brini, M., Chiesa, A., Filippin, L. & Pozzan, T. (1999). Mitochondria as biosensors of calcium microdomains. *Cell Calcium* **26**, 193–199.

Rizzuto, R., Pinton, P., Carrington, W., Fay, F. S., Fogarty, K. E., Lifshitz, L. M., Tuft, R. A. & Pozzan, T. (1998). Close contacts with the endoplasmic reticulum as determinants of mitochondrial Ca^{2+} responses. *Science* **280**, 1763–1766.

Renard-Rooney, D. C., Hajnóczky, G., Seitz, M. B., Schneider, T. G., Thomas, A. P. (1993). Imaging of inositol 1,4,5-trisphosphate-induced Ca^{2+} fluxes in single permeabilized hepatocytes. Demonstration of both quantal and nonquantal patterns of Ca^{2+} release. *Journal of Biological Chemistry* **268**, 23601–23610.

Robb-Gaspers, L. D., Burnett, P., Rutter, G. A., Denton, R. M., Rizzuto, R. & Thomas, A. P. (1998). Integrating cytosolic calcium signals into mitochondrial metabolic responses. *EMBO Journal* **17**, 4987–5000.

Sharma, V. K., Ramesh, V., Franzini-Armstrong, C. & Sheu, S. S. (2000). Transport of Ca^{2+} from sarcoplasmic reticulum to mitochondria in rat ventricular myocytes. *Journal of Bioenergetics and Biomembranes* **32**, 97–104.

Simpson, P. B., Mehotra, S., Lange, G. D. & Russell, J. T. (1997). High density distribution of endoplasmic reticulum proteins and mitochondria at specialized Ca^{2+} release sites in oligodendrocyte processes. *Journal of Biological Chemistry* **272**, 22654–22666.

Simpson, P. B. & Russell, J. T. (1998). Role of mitochondrial Ca^{2+} regulation in neuronal and glial cell signalling. *Brain Research* **26**, 72–81.

Stout, A. K., Raphael, H. M., Kanterewicz, B. I., Klann, E. & Reynolds, I. J. (1998). Glutamate-induced neuron death requires mitochondrial calcium uptake. *Nature Neuroscience* **1**, 366–373.

Szalai, G., Csordás, G., Hantash, B. M., Thomas, A. P. & Hajnóczky, G. (2000). Calcium signal transmission between ryanodine receptors and mitochondria. *Journal of Biological Chemistry* **275**, 15305–15313.

Szalai, G., Krishnamurthy, R. & Hajnćzky, G. (1999). Apoptosis driven by IP_3-linked mitochondrial calcium signals. *EMBO Journal* **18**, 6349–6361.

Wendt-Gallitelli, M. F. & Isenberg, G. (1989). X-ray microanalysis of single cardiac myocytes frozen under voltage-clamp conditions. *American Journal of Physiology* **256**, 574–583.

Wilson, B. S., Pfeiffer, J. R., Smith, A. J., Oliver, J. M., Oberdorf, J. A. & Wojcikiewicz, R. J. (1998). Calcium-dependent clustering of inositol 1,4,5-trisphosphate receptors. *Molecular Biology of the Cell* **9**, 1465–1478.

Acknowledgements

We would like to thank Drs Suresh K. Joseph and Theodore F. Taraschi for comments on this manuscript. This work was supported by a Grant-In-Aid (to G.H.) from the American Heart Association and DK51526 (to G.H.) from NIH. G.H. is a recipient of a Burroughs Wellcome Fund Career Award in the Biomedical Sciences. P.P. is a recipient of a Juvenile Diabetes Foundation Postdoctoral Fellowship.

Corresponding author

G. Hajnóczky: Department of Pathology, Anatomy and Cell Biology, Suite 253 JAH, Thomas Jefferson University, Philadelphia, PA 19107, USA.

Email: gyorgy.hajnoczky@mail.tju.edu